Hriberšek, M., Kulovec, S., & Toubal, L. (2025). Performance Evaluation of Biocomposite Gears Under Fatigue and Wear: Steel Drive Gear Versus Biocomposite Drive Gear and Biocomposite Drive Gear Versus Biocomposite Gear. Fatigue & Fracture of Engineering Materials & Structures, 48(4), 1768-1781. https://doi.org/10.1111/ffe.14590 CC BY 4.0

Fatigue & Fracture of Engineering Materials & Structures

WILEY

FFEMS Fatigue & Fracture of Engineering Materials & Structures

ORIGINAL ARTICLE OPEN ACCESS

Performance Evaluation of Biocomposite Gears Under Fatigue and Wear: Steel Drive Gear Versus Biocomposite Drive Gear and Biocomposite Drive Gear Versus Biocomposite Gear

Matija Hriberšek[1] | Simon Kulovec[2,3] | Lotfi Toubal[4]

[1]Faculty of Polymer Technology (FTPO), Slovenj Gradec, Slovenia | [2]Podkrižnik Group d.o.o., Ljubno ob Savinji, Slovenia | [3]Faculty of Mechanical Engineering, University of Ljubljana, Ljubljana, Slovenia | [4]Department of Mechanical Engineering, Université du Québec à Trois-Rivières (UQTR), Quebec, Canada

Correspondence: Lotfi Toubal (lotfi.toubal@uqtr.ca)

Received: 19 June 2024 | **Revised:** 7 January 2025 | **Accepted:** 17 January 2025

Funding: This work was supported by Natural Sciences and Engineering Research Council of Canada (https://doi.org/10.13039/501100000038) (2460134) and European Union under the European Regional Development Fund (C3330-18-952014).

Keywords: biocomposite gears | failure modes | fatigue | wear

ABSTRACT

Modern trends in using materials for drive applications encourage new research and solutions based on green materials. To expand the use of these materials in specific industrial environments, it is essential to understand their properties, which are determined through basic laboratory tests that simulate the product's real operation. Evaluating the performance of these materials on test specimens and real parts, such as gears, will enable precise optimization for specific applications. This paper presents systematic fatigue and wear characterization of high-density polyethylene (HDPE) reinforced with 30% birch natural wood fibers for selected gear pair cases. The results showed that using the material in combination with a drive steel gear is more desirable than using the same material in a gear pair. The calculated wear coefficient of the biobased composite is comparable to numerical values of wear coefficients for engineering polymer materials.

1 | Introduction

In recent years, the increasing use of materials based on natural ingredients has been encouraged, as they are more environmentally friendly. Using them significantly reduces the harmful impact on the environment, which is in line with sustainable engineering. Unfortunately, most consumer goods are still made from petroleum-based plastics. This raises sustainability issues such as the depletion of nonrenewable resources and pollution, the extent of which is undeniable.

Reinforcement with short natural fibers is proposed to enhance the mechanical properties of low-cost standard plastics and limit their environmental impact. Efforts to produce this type of composite material date back to the 1970s. It was soon realized that the addition of short fibers was necessary to achieve performance comparable to that of engineering plastics, such as nylon [1, 2]. Furthermore, these biocomposites meet the requirements of a circular economy because they are not only recyclable but also retain their mechanical properties after multiple injection cycles [3]. Douglas, Han, and Wang provided technical guidelines with examples of where to use WPC depending on the application case. The authors suggest using these composites in the automotive sector for various technical applications; furniture production; and, in some cases, gearing applications [4].

Summary

- Steel/wood–plastic composite (WPC) has longer durability than WPC/WPC gear pair under fatigue long term.
- Steel/WPC generates low temperatures which is convenient in terms of wear.
- Birch fibers showed positive benefits in terms of mechanical and wear performance.
- WPC showed improved fatigue in comparison to currently available biomaterial.

Although the demand for biocomposite materials has increased over the last decade, so far, only high-strength plastics like nylon and acetal are used for heavy-duty thermoplastic gears in practical applications. These engineering plastics are costly and offer minimal ecological benefits throughout the gear's life cycle compared to other biocomposite alternatives. The main reason for using gears made of nylon or acetal is their high mechanical stiffness compared to other ordinary plastics. The stiffness of the gears ensures efficient torque transmission, prevents flexing, and thus reduces wear. Based on the rigidity requirements of the structure, Young's modulus is used as a criterion to select a material capable of withstanding the bending load while minimizing deformation. Therefore, a more appropriate solution could be to use a common plastic such as polyethylene as a matrix and reinforce it with wood fibers, giving it mechanical properties with comparable or even superior rigidity to engineering plastics, while being more environmentally friendly and cost-effective.

Bravo et al. developed wood polymer composites consisting of HDPE with various weight percentages of birch fibers: 10, 20, 30, and 40 wt%. The authors characterized the composites by determining their tensile and flexural properties and analyzing the damage modes. They concluded that selecting a composite for a particular application requires careful consideration, not only of the mechanical properties but also of the composite's damage process [5]. Sukiman et al. investigated the thermal properties of HDPE reinforced with wood particles at 30–60 wt%. Their findings showed that increasing the wood particle content led to a reduction in thermal conductivity by up to 44% compared to pure HDPE. This highlights the insulating properties of wood particles [6]. Koffi et al. tested the mechanical properties, wettability, and thermal degradation of HDPE reinforced with different percentages of birch fibers [7]. Their findings revealed that birch fiber degrades at a lower temperature than HDPE. Moreover, neither the birch fiber content nor the coupling agent content affects the melting temperature of the material. Furthermore, the tensile strength of composites with 40% birch fibers was more than double that of virgin HDPE. Ezzahrae et al. (2023) tested and evaluated the performance of three wood polymer composites with the same polymer matrix and three different weight contents of wood fibers which were the following: 40, 50, and 60 wt% [8]. They showed that density thermal properties and hardness are proportional to the increased content of wood fibers. They found out that 60% of wood fibers harm the flexural strength, unlike the flexural module which increases it. Askadskii et al. studied wood-polymer composites made with HDPE and various natural fibers to assess their mechanical properties and develop guidelines for semistructural or structural applications [9].

In the context of plastic and biocomposite gears, researchers have investigated their thermal behavior, assessed root stress, and evaluated critical damage mechanisms [10–21]. It has been demonstrated that carbon particles enhance the friction performance of POM gears [14]. However, carbon, unlike short natural fibers, lacks comparable biodegradability benefits. Blais and Toubal tested and validated the mechanical characteristics of HDPE reinforced with short natural fiber using a test bench designed to monitor the high cycle bending fatigue characteristics of gear teeth [15]. Fatigue versus number of cycles was modeled using *S-N* curves, damage indices, and a linearized Weibull distribution. Zorko, Demšar, and Tavčar combined experiments and simulations to evaluate biopolymer gears [16]. By pairing biopolymers with steel gears, they observed lower operating temperatures and wear rates compared to traditional POM and PA plastic gears. Bravo et al. introduced green and biocomposite materials to study gearing fatigue [17]. They evaluated how these gear pairs performed in terms of durability and temperature response under different load conditions. While the study suggests promise for these materials in drivetrain applications, the authors emphasize the need for further research, particularly on wear and fatigue resistance. Hriberšek and Kulovec investigated the performance of steel gear pairs meshed with HDPE composites reinforced with either 20% wt spruce fibers (SFs) or 20% wt beech fibers (BFs) [18]. They found that BFs have a positive impact on the durability and wear resistance of the gears due to their superior mechanical properties. Ghazali et al. analyzed the wear behavior of biopolymer spur gears [19]. They identified the three typical wear stages: running-in, linear, and rapid increase of wear. Their findings demonstrated that biopolymer gears wear similarly to conventional spur gears made from fossil fuel–based polymers. Černe et al. developed a thermomechanical model that produces results consistent with experimental measurements of polymer gear running using high-speed infrared thermography [20]. Černe and Petkovšek implemented a high-speed camera based on optical measurement to evaluate in-mesh tooth deflection analysis of thermoplastic spur gears during running [21].

While some research exists on natural short-fiber composite gears, information remains scarce, limiting the use of WPCs in structural applications. No studies have compared fatigue and wear in steel and biocomposite drive gear configurations. Furthermore, unlike metal gears, WPC gears have lower thermal conductivity, which, combined with friction, can cause heat spikes at their meshing teeth. These characteristics directly influence the progression of wear, often leading to premature failure over time. This wear and thermal degradation are important challenges for WPC gears. It is therefore essential to study the wear and fatigue of WPC gears to facilitate their integration into machine elements.

This paper investigates the fatigue behavior of HDPE reinforced with 30 wt% birch fibers (HDPE BF30). The thermal response of

gear pairs composed of steel meshing with HDPE BF30 (steel/HDPE BF30) and HDPE BF30 meshing with itself (HDPE BF30/HDPE BF30) was characterized. Wear measurements were performed on the tooth flanks of the polymer composite gear to assess its contribution to gear failure. Finally, electron microscopy was used to analyze the damage mechanisms leading to gear failure.

2 | Material and Methods

2.1 | Materials

To produce the pulp required for granule production, short birch fibers were subjected to thermomechanical pulping. The fibers were produced at the Innovations Institute in Ecomatériaux, Ecoproduits et Ecoenergies, Trois-Rivières, Canada, and were dried at 80°C in an air-circulated oven for 24 h, then ground to 20–60 mesh size before use. The fiber aspect ratio (mean length divided by average diameter) classes were obtained by mechanical refining and screening and characterized using an OpTest fiber quality analyzer 5,7. The properties of birch fibers are as follows: the mean length (L) is 0.53 mm, the mean width (D) is 23.8 μm, and the aspect ratio (L/D) is 22.26. Maleic anhydride grafted polyethylene (MAPE) from Eastman as a coupling agent and high-density polyethylene with a melt flow index of 20.0 g/10 min and density of 0.962 g/cm^3 from NOVA Chemicals were used. HDPE pellets were melted on rollers at 170°C, and then, MAPE and fibers were subsequently added according to the desired weight ratio (30 wt%) presented in [7]. The resulting paste was cooled and shredded using an industrial grinder. Granules were then obtained for use in the manufacture of parts, such as, in our case, gears. The mechanical and thermal properties of the material have already been presented in previous works [5, 7].

2.2 | Description of Gear Test Samples

The testing procedure involved two gear pair configurations: (1) steel driving gear paired with a driven gear made of HDPE reinforced with 30% wt of birch short fibers and (2) both gears made of the same material (HDPE reinforced with 30% wt of birch short fibers).

Test gears were produced using a hobbing process, a specialized gear manufacturing technology known for its high degree of dimensional and geometrical precision, as well as for achieving appropriate surface integrity on machined surfaces. These advantages are particularly significant in the automotive industry, where small deviations from the CAD design specification can have significant effects on the gear operating performance and safety. Hobbing is a suitable and flexible machining process for producing small and large numbers of gears with high precision and accuracy. The cutting tool has cutting teeth on a gear blank called a hob. Hobbing is a versatile process that enables machining gears from various materials, such as steel, and polymer-based materials, and can be applied to a wide range of gear modules and types of gear flank: involute, S-gear shape [22]. Spur gear samples were produced using an involute gear hob cutter.

The gears were produced using a CNC hobbing machine center Krauss Maffei KM 50/100 CX. Test gears were produced, specifically 100 specimens, to ensure a stable precision machining process with consistent dimensional quality. The gears were produced using an involute shape of a hob cutter. Table 2 specifies the basic parameters necessary for gear design obtained by contact analysis performed under 0.6 Nm for both gear pairs according to VDI 2736 analytical calculation guidelines. The gear design optimization was done using a specialized analytical calculation procedure the same as Hlebanja et al. used [23].

After machining, the steel gear received superfinishing, a precision surface treatment that utilizes abrasive particles (often ceramic media) to remove burrs and improve surface quality. Superfinishing enhances the gear's functional characteristics by reducing friction, increasing wear resistance, and extending operational life. It is worth noting that both the driving and driven gears share identical geometric and dimensional specifications Table 1.

A 3D coordinate measuring machine assessed the quality of eight teeth on each gear (WPC gear in Figure 1). This assessment assigned a quality class to each tooth according to the ISO 1328-1 standard [24]. This standard defines a gear quality scale from 1 (highest precision) to 12 (greatest deviation from design). Generally, 2–3 quality is characteristic for the reference gears which are treated with polishing. As expected, the WPC gear exhibits lower tooth profile quality compared to the steel gear. The hobbing process of the polymer-based material is characteristic that is subject to greater vibrations and process volatility due to a greater inhomogeneity of the material and lower mechanical properties compared to steel. Furthermore, the WPC's lower thermal conductivity than steel decisively affects the heat removal process from the cutting zone. Usually, poor heat removal

TABLE 1 | Gear parameters and contacting mechanical outputs.

Driving gear/driven gear	Steel/HDPE BF30	HDPE BF30/HDPE BF30
Teeth number, z (–)	20/20	20/20
Gear width, b (mm)	6	6
Normal module, m (mm)	1	1
Pressure angle at normal section, α (°)	20	20
Tip diameter, d_a (mm)	22/22	22/22
Reference diameter, d (mm)	20/20	20/20
Root diameter, d_f (mm)	17.5/17.5	17.5/17.5
Width of the contact (mm)	6/6	6/6
Total overlap ratio under load (–)	2.0	2.1
Length of the contact line (mm)	6.2	6.2
Maximal sliding velocity (m/s)	0.878	0.934
Gear profile quality (ISO 1328, Part 1)	6/11	11/11

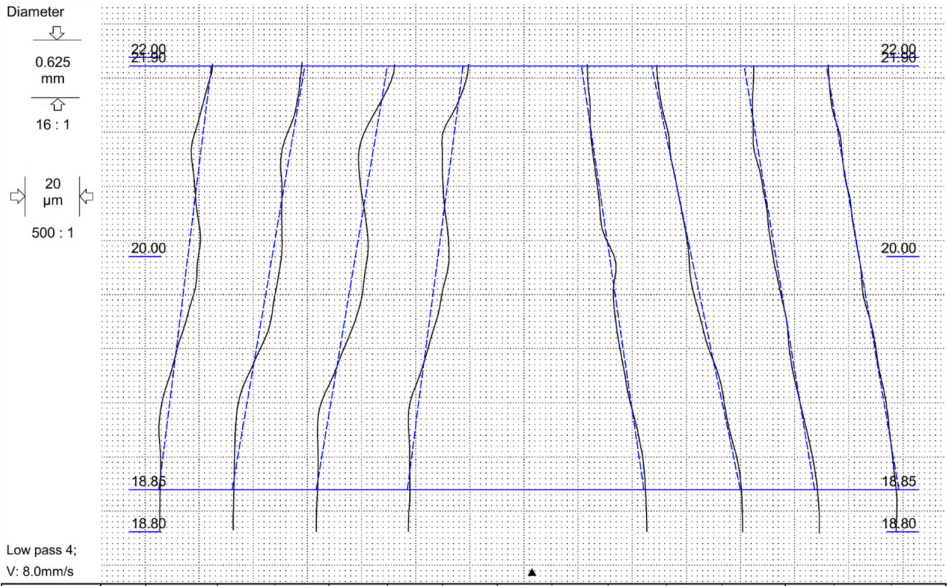

DIN 5480	Q	[...]	x	#16	#11	#6	#1	Tooth	#1	#6	#11	#16	x	[...]	Q
	11	0.0/25.0	23.6	19.5	24.8	28.2	22.0	Fα	21.4	31.1	23.7	25.0	25.3	0.0/25.0	11
!=10 !=10			8.4	8.0	6.8	10.1	8.6	ffα	3.5	4.2	5.0	1.8	3.6		
=11 =11			-23.3	-19.4	-26.9	-26.3	-20.6	fHα	-23.1	-32.8	-26.0	-26.8	-27.2		

FIGURE 1 | Measurement and evaluation of the flank profile of the wood polymer composite gear with CMM. [Colour figure can be viewed at wileyonlinelibrary.com]

results in heat retention in the cutting zone and consequently the formation of a heat-affected area in the material and worse manufacturing tolerances and surface integrity of teeth flanks.

The arithmetical surface roughness (R_a) of the gear tooth flanks was measured three times on four different gear teeth using a surface roughness meter [25]. The first set of measurements recorded the roughness along the gear width. The second set of measurements focused on the gear tooth profile, spanning from the tip to the root diameter. On average, the R_a along the gear width was 1.42 µm, while the R_a for the gear tooth profile was 1.92 µm.

2.3 | Experimental Setup: Fatigue and Thermal Testing

The lifetime tests were carried out with manufactured test gears on a custom test rig (Figure 2). The rig features a rigid cast iron structure that prevents vibrations from the gear pair from reaching the steel table where it is positioned. Rotational motion is transmitted from the motors to the shafts where the gears are mounted via belts and pulleys. Motor 1 drives the rotational motion, while Motor 2 acts as a brake to apply a defined torque on the gears. We measured the torques for each gear pair based on their torsional deformations. To accurately set the center distance between the gear pairs, we incorporated a linear rail into the test rig. This rail lets us adjust the center distance in very fine increments of 0.01 mm. To effectively remove the heat generated during the operation of the motors, two fans were additionally installed on the test rig. The essential technical specifications of the test rig are detailed in reference [18]. We used an infrared camera connected to a PC to monitor the temperature during gear operation. This setup allowed us to see the live temperature distribution on the gear meshing zone. The camera focused on a specific area measuring 2 × 2 mm, with a frame rate of 50 Hz and a display frame rate of 20 Hz.

The experiment was aimed at determining the fatigue life of two gear pairings: steel with HDPE BF30 and HDPE BF30 with HDPE BF30. We tested these under three load conditions (0.6, 0.5, and 0.4 Nm) at a constant speed of 1400 rpm in standard lab conditions. To ensure reliable data, we repeated each experiment three times in the same settings. The last column of Table 2 presents an average value of the achieved number of load cycles with standard deviation for the determined gear pair under the selected load level. The concept of determination of the number of cycles until the gear failure was determined from the diagrams shown in Figure 4 and coincided with the temperature peak at the end. The initial load of 0.6 Nm was chosen based on preliminary contact analysis using the computational software KISSsoft according to calculated method VDI2736, Part 2 [26]. The initial durability tests at 0.6 Nm provided valuable insights. Based on these results, it was designed additional load conditions to explore the full range of the gears' finite life fatigue strength, from about 0.1 million to 5–6 million load cycles. This range is crucial, as even small load variations can significantly affect the gear pair's material behavior. Table 2 summarizes the subsequent durability tests with given operating parameters, including both gear pairs and the average load cycles applied to each. The axis distance between tested gear pairs was 20.0 mm, considering 0.25-mm clearance between teeth to prevent gear collision during meshing due to thermal dilatations.

2.4 | Measurements of Flank Wear

To measure the wear of the HDPE-BF30 gear in both options (steel/HDPE-BF30 and HDPE-BF30/HDPE-BF30), a

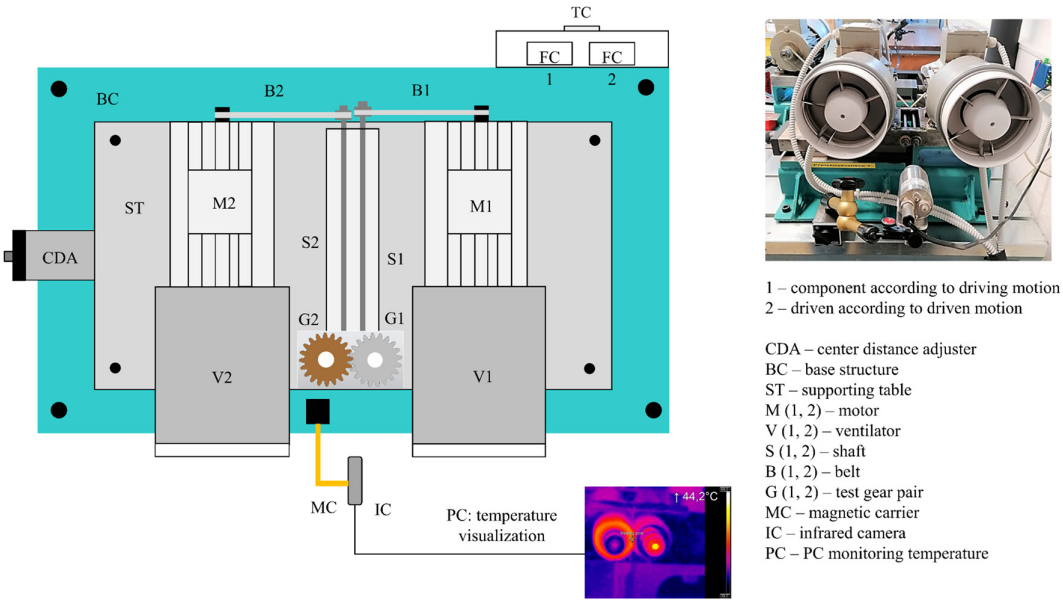

FIGURE 2 | Test rig for fatigue evaluation of polymer gear pairs. [Colour figure can be viewed at wileyonlinelibrary.com]

TABLE 2 | Operating conditions and calculated gear strength.

Gear pair	Rotational speed, n (min^{-1})	Torque, T_d (Nm)	Repetitions	The average number of load cycles, $N{\cdot}10^6$ (–), (std dev 10^6) (–)	Hertzian pressure, σ_H (MPa)	Tooth root stress, σ_F (MPa)
Steel/HDPE BF30	1458	0.6	3	0.3 (0.01)	47.5	27.0
HDPE BF30/ HDPE BF30				0.4 (0.09)	25.4	20.8
	1465	0.5	3	0.7 (0.06)		
				1.1 (0.3)		
	1472	0.4	3	6.2 (0.3)		
				3.3 (1.0)		

3D optical microscope Alicona InfiniteFocus SL was used [27] to measure the tooth flank profile before and after testing (Figure 3a). Wear was measured on a marked tooth of the wood polymer composite gear after each test stop to track its wear behavior over time. To maintain consistent testing conditions, the contact area between the driving and driven gears at each stop was marked, allowing us to resume testing under identical conditions. After testing, a cloud of points in ASCII files for each tooth profile was imported and processed into the computing software for 2D drawing and measuring where wear measurements at defined points at gear circle diameters were taken and compared to the referenced unworn tooth profile [28]. The optical measurement process was performed each time using 10× magnification of the image. A spot-measuring area was defined as 2×10 mm, depending on the tooth size (Table 3). The optical system had a resolution of 100 nm in the vertical direction and 4 μm in the lateral direction. The contrast of the monitored image was 1, and the exposure time was 1.4 ms. Figure 3b presents a 3D-scanned part of the worn tooth. The image was generated using software from the optical scanner. Figure 3c. shows scanned results in the form of a merged cloud of points that illustrates an example of a worn tooth profile on which wear measurements were taken.

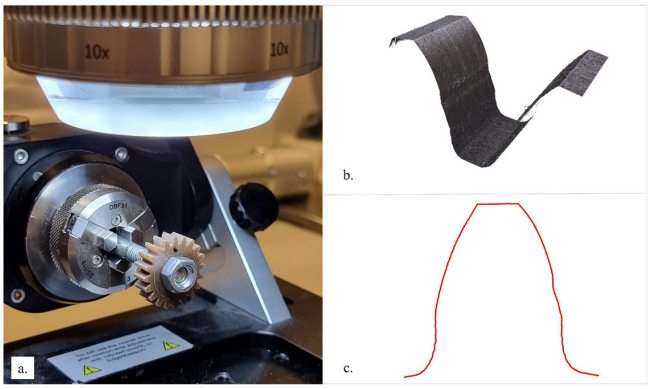

FIGURE 3 | (a) Optical scanning of test gear. (b) Schematic 3D illustration of the scanned test gear. (c) Processed tooth profile in 2D plane. [Colour figure can be viewed at wileyonlinelibrary.com]

TABLE 3 | Settings used of Alicona InfiniteFocus SL.

Zoom lens	10×
Operating area of measuring device (*X*, *Y*, *Z*) (mm)	50×50×155
Operating area of lens (mm)	2×2
Maximal lateral resolution (μm)	1.76
Maximal vertical resolution (nm)	100
Minimal measurable profile roughness R_a (μm)	0.3
Minimal measurable surface roughness S_a (μm)	0.15
Minimal measurable radius (μm)	5

3 | Theoretical Framework and Calculations for Evaluating Abrasive Wear

One of the main aims of the research was to precisely determine the wear resistance of the observed biobased composite material on the example of use in gears. By the VDI 2736 Part 2 guideline, the permissible linear wear W_{zul} is defined by Equation (1):

$$W_{zul} = (0.1 \ldots 0.2) \cdot m_n. \tag{1}$$

Depending on the tooth root failure, which is a characteristic failure mechanism when a steel/polymer gear pair is analyzed, it is necessary to consider the wear rate of the tooth flanks and compensate it with a safety factor when calculating permissible root stress. To conduct precise calculations for load-carrying capacity in KISSsoft, it is appropriate to consider the wear of observed wood composite gear. In the absence of an international ISO standard specifically for the design of polymer gears, the VDI 2736 guideline is widely adopted as a reference in both research and industrial settings. According to VDI 2736 guideline, a procedure for abrasive wear evaluation of polymer gears is proposed. This type of wear occurs when gears run dry. The average linear wear W_m is defined by

$$W_m = \frac{T_d \cdot 2 \cdot \pi \cdot N \cdot H_V \cdot k_W}{b \cdot z \cdot l_{Fl}}. \tag{2}$$

The degree of tooth loss H_V is

$$H_V = \frac{\pi \cdot (u+1)}{z_2 \cdot cos\beta_b} \cdot \left(1 - \varepsilon_1 - \varepsilon_2 + \varepsilon_1^2 + \varepsilon_2^2\right), \tag{3}$$

where $u = 1$ is the gear ratio, $z_2 = 20$ stands for the number of teeth (wood composite gear), and $\beta_b = 0$ (°) is the helix angle at the base circle.

The partial contact ratios ε_1 of the driver and ε_2 of the driven gear can be calculated with Equation (4):

$$\varepsilon_i = \frac{z_i}{2 \cdot \pi} \cdot \left(\sqrt{\left(\frac{d_{ai}}{d_{bi}}\right)^2 - 1} - tan\alpha \right), \tag{4}$$

where $z_{1,2} = 20$ are numbers of teeth, $d_{a1,2} = 22$ mm addendum circle diameters, $d_{b1,2} = 18.794$ mm base circle diameters, and $\alpha = 20°$ operating pressure angle in the transverse section.

The profile line length of the active tooth flank l_{Fl} is calculated from Equation (5) [4]:

$$l_{Fl} = \frac{1}{d_b} \cdot \left(\left(\frac{d_{Na}}{2}\right)^2 - \left(\frac{d_{Nf}}{2}\right)^2 \right), \tag{5}$$

where $d_{Na} = 21.979$ mm stands for the active tip diameter and $d_{Nf} = 18.927$ mm for the active root diameter [26].

4 | Results and Discussion

4.1 | Fatigue Testing

Figure 4 shows the average surface temperature variation over the number of loading cycles for the three torque levels, obtained using an IR camera. The temperature profiles focus on the gear mesh–tooth area, which is the likely failure zone. During the running-in phase, the meshing temperature gradually increases until it stabilizes, indicating that the wood polymer composite gear teeth are adapting to the driving gear teeth. As the gears continue running, a stable meshing temperature is maintained, leading to wear. In the final phase, increasing temperature fluctuations can trigger fatigue-induced cracks, ultimately leading to the failure of the first tooth.

Experiments revealed that the WPC/WPC gear pairing had the most significant temperature amplitude fluctuation during the running at all three torque levels. From a friction perspective and wear abrasion, using the same material for both gears is not ideal because it leads to more friction at the contact point due to the tendency of materials to weld. This friction generates more heat, resulting in higher temperatures; faster wear; and ultimately, earlier gear failure, as research suggests [29].

Under the higher and medium torques, the WPC/WPC gear pair reaches longer durability life due to the higher capability of the gear flank profile adaptation which results in greater contact surface and consequently lower root stresses. By reducing the load on the gear pair, the durability of the test increases over the lifespan, which highlights the increased occurrence of abrasive wear on the tooth flanks which is narrowly connected with appropriate friction contact between two paired materials. This increased friction might also explain the larger temperature fluctuations observed in the WPC/WPC tests. Interestingly, the steel/WPC gear pairing showed a longer lifespan at the 0.4-Nm torque level. This is likely due to better tribological contact conditions and a lower friction coefficient, which becomes a more critical factor during longer fatigue tests. In all three experiments, the meshing temperatures were consistently lower for the steel/WPC gear pairing. This suggests more favorable tribological contact conditions between the driving and driven gears, potentially due to a lower friction coefficient.

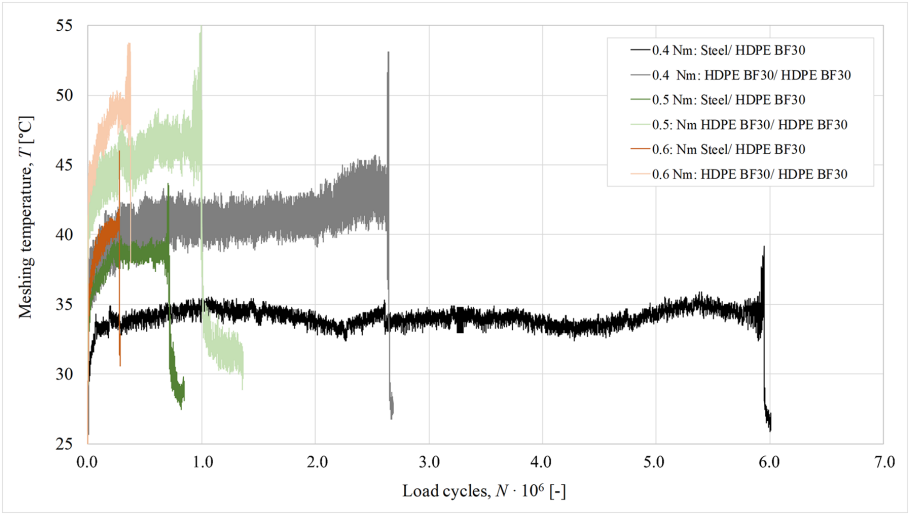

FIGURE 4 | Meshing temperature in dependency of load cycles. [Colour figure can be viewed at wileyonlinelibrary.com]

4.2 | Wear Evaluation

To understand how different gear materials wear, there was analyzed steel/HDPE BF30 and HDPE BF30/HDPE BF30 pairs throughout their lifetime during testing. This analysis will help us define each gear combination's precise fatigue characteristics (*S*-*N* lines). The previous fatigue tests provided a good baseline at specific torques. To simulate a longer operating life (5–10 million cycles), wear at 0.4-Nm torque was analyzed.

4.2.1 | Steel/HDPE BF30

Figure 5 shows the relationship between meshing temperature and fatigue cycles (upper chart) and average flank wear versus fatigue cycles (lower chart) for the gear pair (steel/HDPE BF30). Wear was measured at key points throughout the gear pair's lifetime, including the running-in phase, wear-in phase, crack occurrence, and crack progression. These stages occur when at least one gear is made of WPC. The first measurement was taken just after the running-in phase to assess its impact on WPC gear wear. The end of the run-in phase was empirical, based on meshing temperature stabilization after the initial transient increase. During the wear-in phase, meshing temperature stabilizes, with small variations until the final phase, where initial cracks in the tooth roots lead to tooth failure.

The chart in Figure 6 displays the measured flank wear of a wood–polymer composite gear, indicating its position along the height of the gear tooth (as shown on the right side of Figure 6). Each line represents a different measurement, distinguished by color, to illustrate wear progression over the entire lifespan of the wood composite gear. The wear at each position along the tooth height was calculated by comparing the linear tooth width of the new/referenced profile with the worn profile at specific diameters, which are also depicted on the right side of Figure 6. To correctly evaluate the wear of the gear profile, it is necessary to overlap the tooth profiles on the tip diameter. Due to the deformation of the teeth, there is a geometric deviation between the profiles in the nonactive root region.

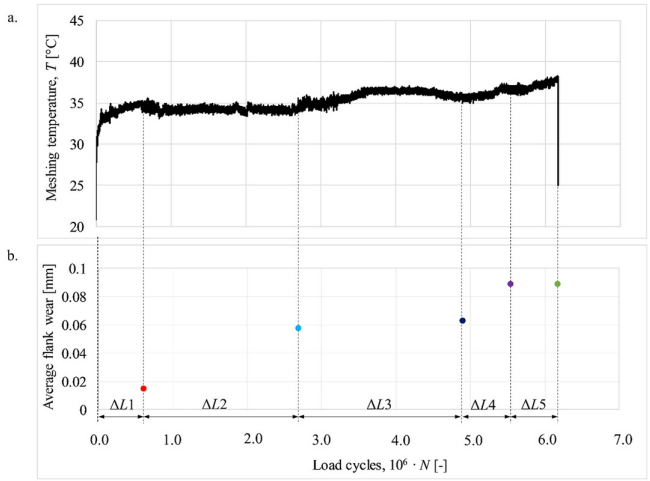

FIGURE 5 | Temperature in dependency of steel/HDPE BF30 gear pair cycles produced under load 0.4 Nm with associated measurements of average flank wear of observed tooth on HDPE BF30 gear. [Colour figure can be viewed at wileyonlinelibrary.com]

For wear occurrence, two prominent areas with increased wear are evident: one around the reference/pitch diameter and the other around the base diameter. The increased wear near the reference diameter is attributed to the maximum amplitude of Hertzian pressure distribution caused by the driving steel gear on the wood composite gear, resulting in a higher wear rate.

A large contribution of abrasive wear can be detected in the area of the base circle, mainly due to the changed contact conditions that occur after the running-in phase of the gear pair. It results in the plastic gear deforms and thus increases the sliding during the engagement. Sliding flanks cause the formation of abrasive wear on the less resistant gear material. Another reason for composite flank wear presents unmodified steel and composite tooth profiles, which could be attributed to the lack of modifications in the tip and root relief. Consequently, there is not a fully smooth transition of stress distribution, leading to a higher

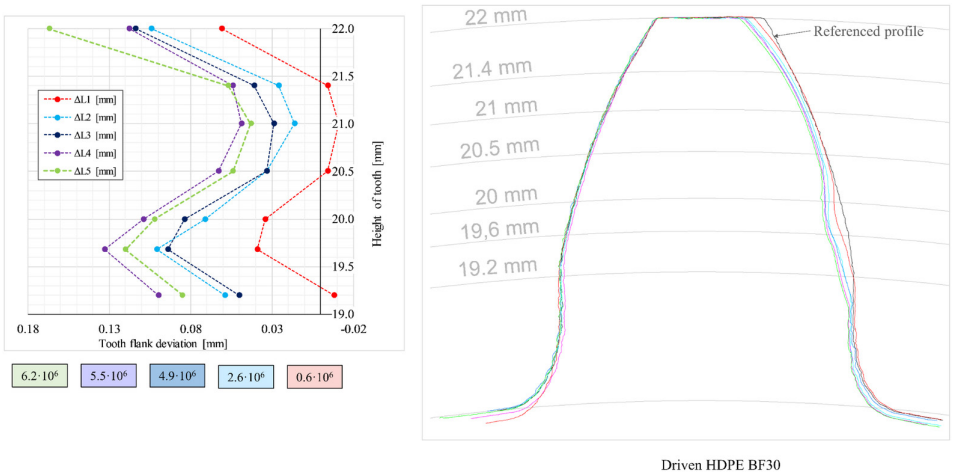

FIGURE 6 | A detailed presentation of wear progression at selected gear diameter measuring points through test duration valid for steel/HDPE BF30 gear pair exposed load 0.4 Nm. [Colour figure can be viewed at wileyonlinelibrary.com]

TABLE 4 | Wear evolution of the driven gear at measured gear diameters—final (fifth) phase (steel/HDPE BF30).

Gear diameter	19.2	19.68	20.0	20.5	21.0	21.4	22.0
Flank wear (mm)	0.085	0.120	0.102	0.054	0.043	0.057	0.167

wear rate through the entire height of teeth. It is proven also by Table 4 which presents cumulative flank wear contribution at certain gear diameters.

4.2.2 | HDPE BF30/HDPE BF30

Figure 7 shows the relationship between meshing temperature and fatigue cycles (upper chart) and average flank wear versus fatigue cycles (lower chart) for the gear pair (HDPE BF30/HDPE BF30). The same phenomena observed previously are also observed here (Cf. 4.2.1 steel/HDPE BF30).

Figure 8 shows how the wear on the driven HDPE BF30 gear teeth increases with the number of load cycles. Wear was measured under the same conditions as the steel/HDPE BF30 gear pair. Unlike the WPC gear shown in Figure 6 (right figure), the wear on this gear is evenly distributed along the entire tooth height. By comparing the average wear as a function of the number of load cycles reached for the two pairs of gears (steel/HDPE BF30, Table 4, and HDPE BF30/HDPE BF30, Table 5), it can be concluded that the gear pair comprised of the same material achieved less wear but lasts a shorter time despite the occurrence of a similar wear distribution trend across the tooth height. However, the reason for the shorter lifetime of the gear pair which is comprised of HDPE BF30/HDPE BF30 can be potentially due to unfavorable contact conditions that become more pronounced during long-term operation (several million cycles). This is also proven by the higher meshing temperatures of 17% in comparison to meshing temperatures which occur in the contact between steel and HDPE BF30 gear pair.

After each 3D optical scanning process of the worn tooth flank, the gear tooth was also examined under an optical microscope.

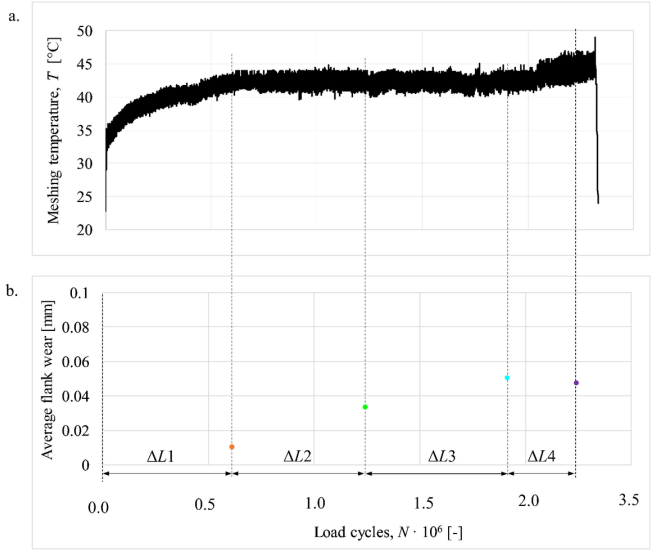

FIGURE 7 | Temperature in dependency of HDPE BF30/HDPE BF30 gear pair cycles produced under load 0.4 Nm with associated measurements of average flank wear of observed tooth on HDPE BF30–driven gear. [Colour figure can be viewed at wileyonlinelibrary.com]

Figure 9 presents images captured with an optical microscope [28], at a magnification of 5×. Each image illustrates characteristic damage contributing to the eventual gear tooth failure. In the image of the referenced gear (Figure 9a), some burrs and traces resulting from the cutting process, particularly from the hob cutter, are visible. This cutting process involves localized material destruction, leading to the possibility of fiber appearance on the gear flank surface due to the failure of cohesion between fibers and matrix during the cutting process of the composite

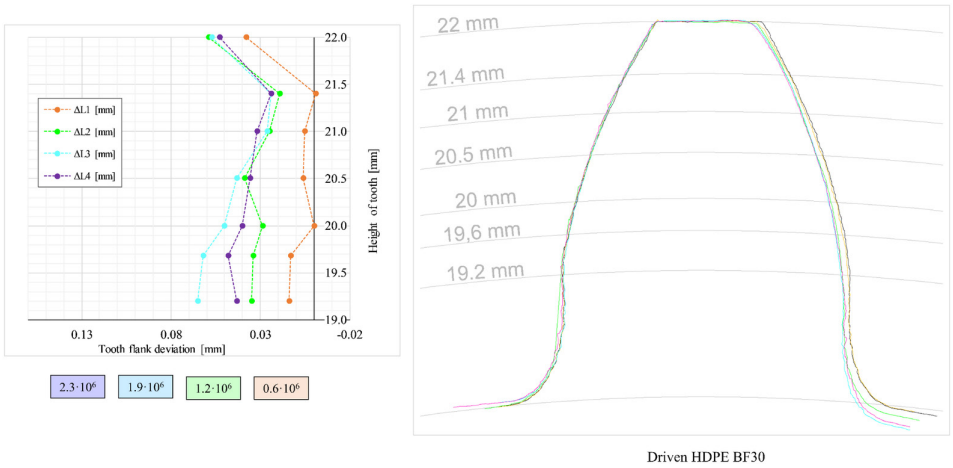

FIGURE 8 | A detailed presentation of wear progression at selected gear diameter measuring points through test duration valid for HDPE BF30/HDPE BF30 gear pair exposed load 0.4 Nm. [Colour figure can be viewed at wileyonlinelibrary.com]

TABLE 5 | Wear evolution of the driven gear at measured gear diameters—final (fifth) phase (HDPE BF30/HDPE BF30).

Gear diameter	19.2	19.68	20.0	20.5	21.0	21.4	22.0
Flank wear (mm)	0.043	0.048	0.040	0.036	0.032	0.024	0.055

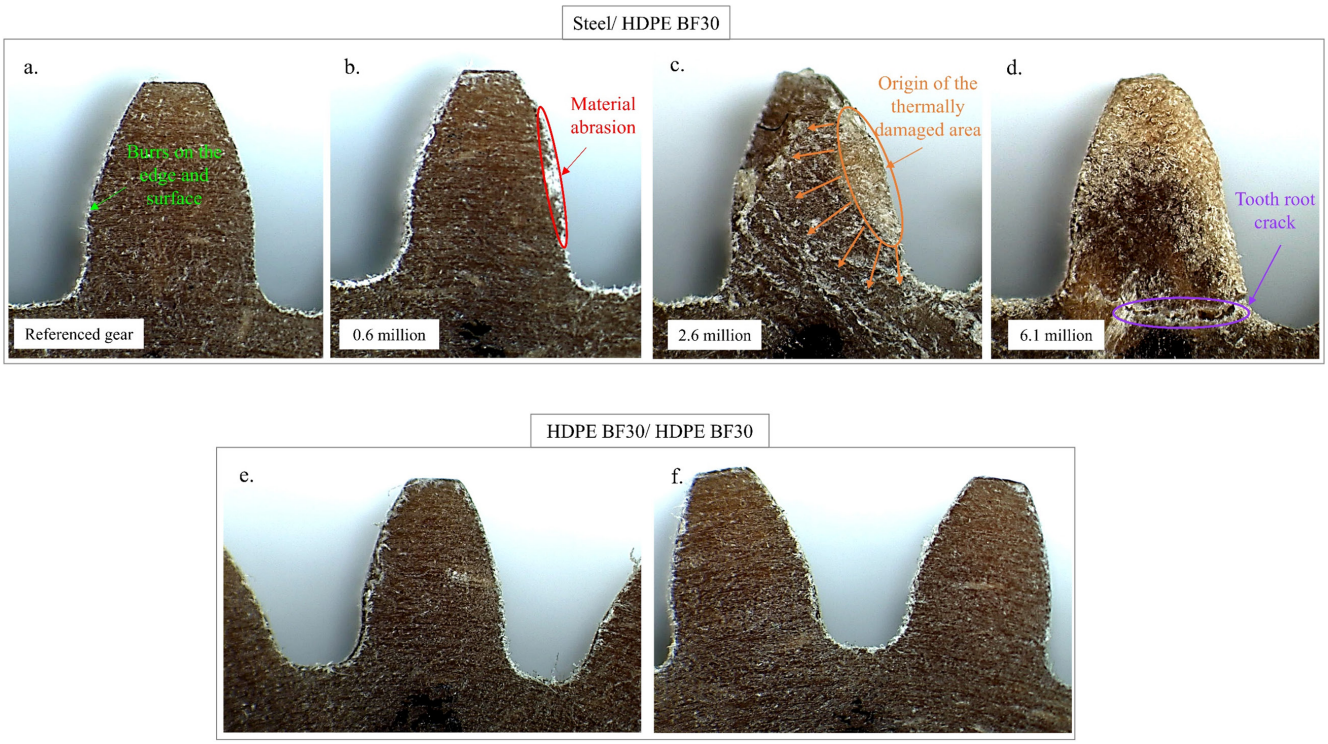

FIGURE 9 | Steel/HDPE BF30. (a) Referenced gear tooth. (b) Wear mechanism: abrasive effect. (c) Thermally damaged area. (d) Tooth root crack. HDPE BF30/HDPE BF30 exposed load 0.4 Nm. (e) Driving gear. (f) Driven gear. [Colour figure can be viewed at wileyonlinelibrary.com]

material. The image in Figure 9b is captured just after the running-in phase of the observed gear pair. The increased material damage, seen in the form of a damaged flank surface around the reference diameter, indicates increased abrasive wear resulting from tooth adaptation between the harder-driving steel gear and the HDPE BF30–driven gear. This material damage occurs in the area around the reference diameter where maximal contact pressure is known to occur during gear pair meshing. In Figure 9c, taken during the wear-in phase, the microscope image highlights an orange ellipse, indicating a locally affected thermal zone that occurred after 2.6 million load cycles. No more visible chipping of material particles on the tooth flank is

detected. At this point, a large area of the heat-affected zone is formed, illustrated by the orange-marked ellipse. The origin of the zone is conditioned by the formation of maximum Hertzian pressure, which appears on the reference circle (Figure 9c: material abrasion) and long-term fatigue running. The heat accumulates and spreads inside the tooth due to the poor thermal conductivity of the material. When the thermal damage of the area extends to the root area, the tooth cracks appear and cause the beginning of the failure.

The final image (Figure 9d) was captured just before the complete tooth root failure. This phase reveals a significant thermally damaged area, indicative of a generalized thermal failure in the gear teeth. Additionally, the image displays a prominent crack at the tooth root, which will ultimately lead to the gear's fracture.

Figure 9e shows the driving HDPE BF30 gear, and Figure 9f depicts the driven HDPE BF30 gear after 2.3 million load cycles under 0.4 Nm.

Table 6 displays the calculated wear coefficients according to VDI 2736 guidelines for driven gear produced from HDPE BF30 material. These coefficients were calculated based on the average linear wear measured from Figure 6 and 8 specific numbers of load cycles for each gear pair combination.

In the case of a combination where the same material is used, faster failure occurs, which has been already explained in the previous section. The reason for faster gear-tooth failure is the nonoptimal tribological contact conditions because the same materials have the tendency to be welded which invokes a higher amount of friction force and consequently contact temperature fluctuation. It results in faster weakening of the material's mechanical properties and, consequently, premature failure.

For the steel/HDPE BF30 gear pair, a significant increase in the wear coefficient is observed during the final running phase, coinciding with the appearance of the first cracks at the tooth root due to fatigue. This suggests increased gear tooth deformation and alters contact conditions, leading to higher gear contact temperatures. Additionally, the average wear coefficient is calculated for each gear pair to allow comparison with traditional polymer-based materials (Table 6). The wear coefficient distribution over the operating period differs between the two gear combinations. In the steel/HDPE BF30 case, the maximum wear coefficient occurs after the end of the run-in phase. This phase is characterized by deformation and, consequently, adaptation of the polymer composite tooth flanks due to the action of the more mechanically resistant steel driving gear, which essentially shapes the softer WPC gear.

In the following, where the operation of the steel/ HDPE BF30 gear transmission enters the wear-in phase, the wear coefficients decrease and stabilize around the value $5{\cdot}10^{6}$–$6{\cdot}10^{6}$ mm^3/Nm. The wear resistance of the material is similar until gear failure. It indicates stabilized conditions during the whole period of the operational phase which is a positive benefit of the implemented biobased composite in the steel/HDPE BF30 gearing case. The mentioned is considered a positive fact since the wear coefficient does not increase significantly in the last phase of operation, where pronounced fatigue effects appear. This information indicates a positive influence on the mechanical properties of the fibers in the polymer matrix, which significantly increases the rigidity of the structure and

TABLE 7 | The current state of the art on calculated wear coefficients according to VDI 2736-2 for various material gear pairs during dry running [18, 28].

	Wear coefficient k_w 10^{-6} (mm^3/Nm)	R_a (μm)
Biobased plastics		
Steel/HDPE SF20 [18]	32.8	0.96
Steel/HDPE BF20 [18]	19.1	2.06
Engineering plastics		
Steel/POM [28]	7.91	0.50
Steel/PA66 [28]	43.5	0.40
Steel/PA66 CF20 [28]	5.39	0.45

TABLE 6 | Calculated wear coefficients according to VDI 2736-2 with dry running obtained by the presented research.

Gear pair (driving/driven)	Number of load cycles N (–)	Wear coefficient k_w 10^{-6} (mm^3/Nm)	Average k_w 10^{-6} (mm^3/Nm)	The average R_a (std dev) (μm)
Steel/HDPE BF30	612.590	9.61	6.96	1.42 (0.25)
	2.693.333	8.38		
	4.890.410	5.01		
	5.538.341	6.22		
	6.168.602	5.58		
HDPE BF30/HDPE BF30	612.590	6.74	9.06	1.42 (0.25)
	1.236.960	10.68		
	1.914.343	10.26		
	2.317.580	8.57		

dimensional stability. Because the wear coefficient did not increase significantly just before the failure of the gear, it can be concluded that the dominant failure mechanism in the given case was long-term fatigue.

Higher wear coefficients are visible in the gear pair where the same material was used. The value trend is different from the previous case for steel/HDPE BF30 because, during the operation phase, the coefficient increases randomly. The reason for the result should be in undesirable tribological conditions between the same used material for driving and driven gear which also refers to the basic guideline VDI2736 [26]. More suitable tribological contact could have a more positive effect on the material degradation effect during long-term fatigue which is expressed in longer durability for the steel/HDPE BF30 gear pair.

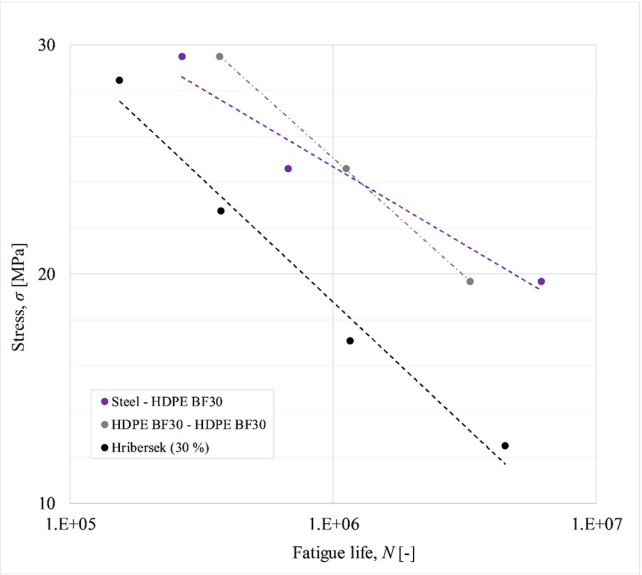

FIGURE 10 | Comparison of gear tooth lifetimes measured in this study and previously by Hriberšek and Kulovec [18]. [Colour figure can be viewed at wileyonlinelibrary.com]

Gear results presented in Table 7 had the same geometry as the gears presented in this paper. The manufacturing process of the presented gear results in Table 7 was also the same as for the observed gears in this paper. The values for abrasive wear coefficients were obtained by the same measuring abrasive wear protocol. The arithmetical surface roughness R_a listed in Table 5 is considered along tooth width. From Table 7, it can be concluded that the implemented new biobased material is suitably wear-resistant, in the case of permissible stresses that occur for the mentioned material in the root of the tooth. In the field of comparison between the mentioned material and in the case of similar types of materials which are HDPE reinforced with SFs and BF presented in Table 7 (HDPE SF30), it has a promising future in terms of wear resistance to continue its research work with aim to integrate it in practical engineering cases.

4.3 | Fatigue Evaluation

Figure 10 presents *S-N* lines for steel/HDPE BF30 and HDPE BF30/HDPE BF 30. Each *S-N* line was calculated using an analytical program according to the VDI 2736 guideline. To precisely calculate the *S-N* line, input parameters in the form of mechanical properties were characterized such as modulus elasticity, tensile strength, and strain at break and parameters connected with durability experiments, specifically torque, rotational speed, number of load cycles, and typical

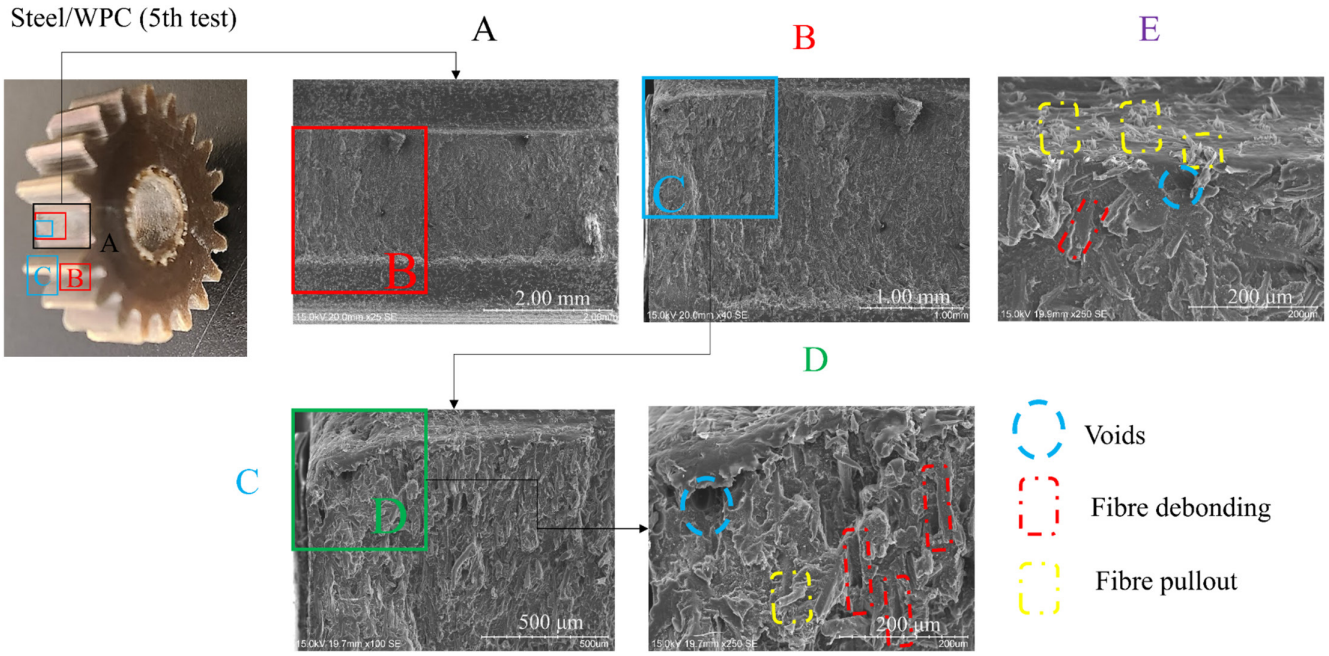

FIGURE 11 | Wood polymer composite gear observed in the gear pair (steel/WPC) at the fifth test referring to Figure 8 (green point data). [Colour figure can be viewed at wileyonlinelibrary.com]

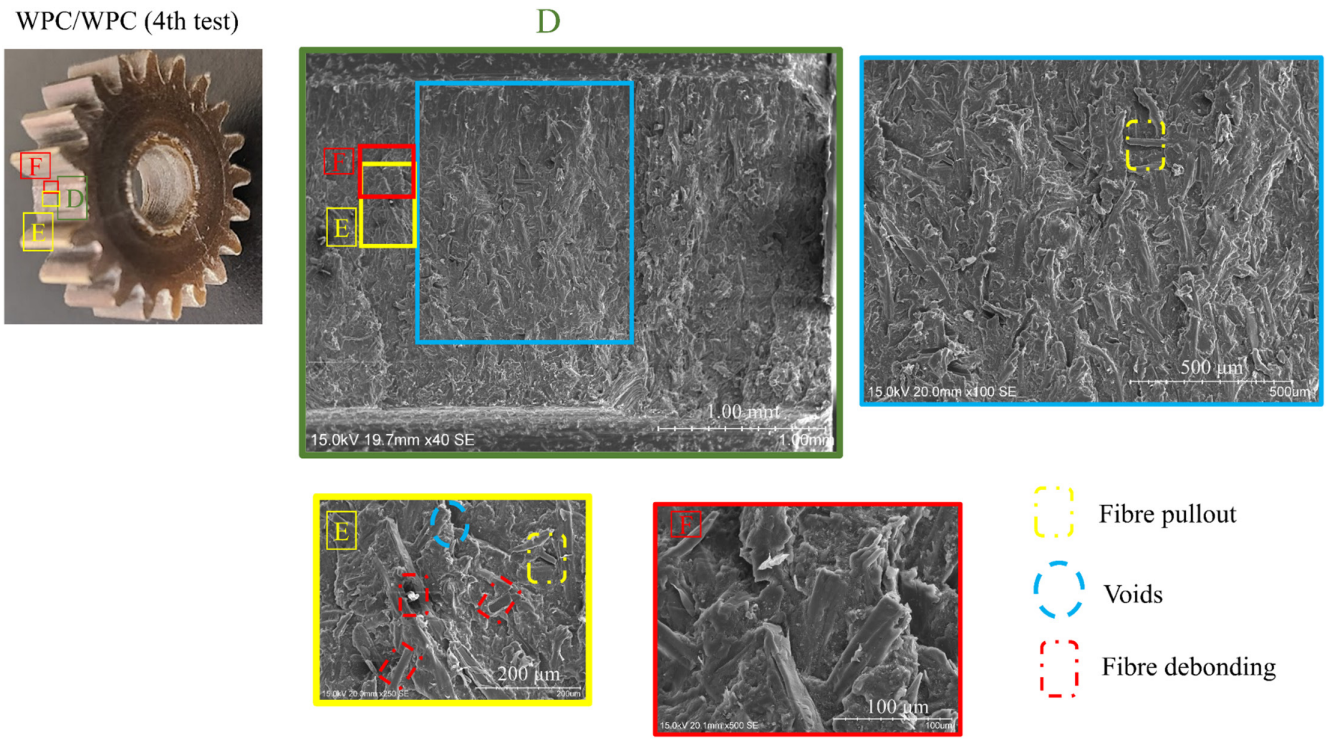

FIGURE 12 | Wood polymer composite gear observed in the gear pair (WPC/WPC) at the fourth test referring to Figure 8 (green point data). [Colour figure can be viewed at wileyonlinelibrary.com]

gear failure mechanism which was tooth failure. As was already presented in the form of temperature-load cycle diagrams in Figure 4, *S-N* lines prove the durability resistance in gear tooth root of each material observed in each gear pair. At higher load levels, a slightly better material fatigue resistance can be reached in gear pair HDPE BF30/HDPE BF30. At lower load levels, HDPE BF30 meshed with driving steel gear shows higher tooth root stress and consequently longer durability performance. Presented results in this research are added to past references cited from the paper by Hriberšek and Kulovec [18]. It is seen that the observed material with birch fibers has better root fatigue resistance in comparison to the similar compounded material but with BFs which also proves the promising mechanical ability of birch fibers to be implemented and observed for further research.

4.4 | SEM Microscopy

Figures 11 and 12 depict the fractured surface of the composite, with scanning electron microscopy images illustrating the state of HDPE-based composite surface at magnifications up to 250×.

The matrix deformation is initiated in the up area parallel to the gear tooth flank, while the rest of the image portrays a flat surface (Figure 11 A). This suggests that the complete matrix rupture occurred after an initial plastic deformation. Twists and bent material at the matrix level are observable, indicating signs of plasticity or permanent material deformation. Additionally, surface holes and fiber/matrix decohesion are evident, suggesting fiber pull-out (Figure 12 E and D).

5 | Conclusions

The paper presents two different gear combinations (steel/HDPE BF30 and HDPE BF30/HDPE BF30) and their detailed fatigue and thermal responses in the meshing zone. Additionally, the wear resistance of the presented biobased composite material was measured under various torques (0.6, 0.5, and 0.4 Nm). From the research, the following conclusions can be reached:

- Based on the measured duration of the combinations, it was found that the combination with a steel gear achieves a longer duration at a lower torque of 0.4 N where contact pressure and root stresses are lower which means longer test and more expressed fatigue phenomena.
- At higher torques (0.6 and 0.5 Nm), both combinations are similar with a slightly longer lifespan from the HDPE BF30/HDPE BF30 combination.
- It was found that the selection of material for the driving and driven gears is crucial, as it indirectly affects the development of contact temperature during engagement. It turned out that a gear pair made of the same material exhibits significantly higher contact temperatures, which is a consequence of excessive friction between the materials due to the tendency to weld and negatively affects the engagement process.
- The thermal response from the meshing zone can be potentially correlated with abrasive flank wear. The measured linear wear depending on the obtained number of cycles under the prescribed torque refers to lower material wear coefficients for the steel/HDPE BF30 gear pair which is important engineering data when the dominant mechanism of tooth failure is wear.

- Comparing wear coefficients between HDPE BF30 material and engineering plastics from which the gears were produced by the same manufacturing protocol and measuring wear, it can deduce very promising results in terms of excellent wear resistance of the presented material in this research.
- There is also progress in the modeled *S-N* curve compared to the results of testing gears with the same matrix and the same percentage of other types of fibers (beech) since the presented material exceeds the existing stresses of materials from the literature.
- Failure mode of the HDPE BF30 gears was tooth root fracture which is the most common mode when the polymer-based gears are tested on long fatigue term. SEM analysis clearly presents classic mechanisms of composite fractures which are related on the relation between matrix and fibers, such as fiber pull-out and fiber debonding.

Nomenclature

b (mm)	gear width
D (mm)	fiber width
d (mm)	reference diameter
d_a (mm)	tip diameter
d_{b1} (mm)	base circle diameter
d_f (mm)	root diameter
d_{Na} (mm)	active tip diameters
d_{Nf} (mm)	active root diameter
f (Hz)	frequency
H_V (–)	degree of tooth loss
k_w (10^{-6} mm^3/Nm)	wear coefficient
L (mm)	fiber length
l_{Fl} (mm)	line length of active tooth flank
m (mm)	normal module
N (–)	number of cycles
n (min^{-1})	rotational speed
P (kW)	power
R_a (μm)	arithmetical surface roughness
T_d (Nm)	torque
U (V)	voltage
W_m (mm)	linear wear
W_{zul} (mm)	permissible linear wear
z (–)	tooth number
α (°)	pressure angle at normal section
ε (–)	contact ratio
σ (MPa)	stress
σ_F (MPa)	tooth root stress
σ_H (MPa)	Hertzian pressure
Φv (m^3/s)	volume flow

Author Contributions

Matija Hriberšek: conceptualization, methodology, validation, formal analysis, writing – original draft. **Simon Kulovec:** project administration, funding acquisition. **Lotfi Toubal:** project administration, funding acquisition, conceptualization, methodology, formal analysis, writing – review and editing.

Acknowledgments

This work was supported by the Republic of Slovenia the European Union under the European Regional Development Fund (Grant Number C3330-18-952014). The authors would like to thank Prof. Demagna Koffi from the Université du Québec à Trois-Rivières for his assistance in material manufacturing.

Data Availability Statement

The data that support the findings of this study are available from the corresponding author upon reasonable request.

References

1. J. F. Siau and J. A. Meyer, "Wood-Polymer Composites: New Materials With Unique Physical Properties," *Studies in Conservation* 23 (1978): 11–14.

2. B. V. Kokta, R. Chen, C. Daneault, and J. L. Valade, "Use of Wood Fibers in Thermoplastic Composites," *Polymer Composites* 4 (1983): 229–232.

3. A. Bourmaud and C. Baley, "Rigidity Analysis of Polypropylene/Vegetal Fibre Composites After Recycling," *Polymer Degradation and Stability* 25 (2009): 297–305.

4. J. G. Douglas, Y. Han, and L. Wang, "Wood–Plastic Composite Technology," *Current Forestry Reports* 1 (2015): 139–150.

5. A. Bravo, L. Toubal, D. Koffi, and F. Erchiqui, "Development of Novel Green and Biocomposite Materials: Tensile and Flexural Properties and Damage Analysis Using Acoustic Emission," *Materials and Design* 66 (2015): 16–28.

6. M. S. Sukiman, T. Kanit, F. N'Guyen, A. Imad, and F. Erchiqui, "On Effective Thermal Properties of Wood Particles Reinforced HDPE Composites," *Wood Science and Technology* 56 (2022): 603–622.

7. A. Koffi, F. Mijiyawa, D. Koffi, F. Erchiqui, and L. Toubal, "Mechanical Properties, Wettability and Thermal Degradation of HDPE/Birch Fiber Composite," *Polym.* 13 (2021): 1–15.

8. M. F. Ezzahrae, A. Nacer, E. Latifa, Z. Abdellah, I. Mohamed, and J. Mustapha, "Thermal, and Mechanical Properties of a High-Density Polyethylene (HDPE) Composite Reinforced With Wood Flour," *Mater Today Proceed.* 72 (2023): 3602–3608.

9. A. Askadskii, T. Matseevich, A. Askadskii, P. Moroz, and E. Romanova, *Structure and Properties of Wood-Polymer Composites (WPC)* (United Kingdom: Newcastle upon Tyne: Cambridge Scholars Publishing, 2019).

10. O. Faruk, R. A. Hickock, and L. M. Matuana, "Polybutene as a Matrix for Wood Plastic Composites," *Composites Science and Technology* 70 (2010): 167–172.

11. A. Pogacnik and J. Tavcar, "Accelerated Testing and Temperature Calculation of Plastic Gears," *Gear Solutions* 15 (2016): 34–40.

12. C. Hasl, H. Liu, P. Oster, T. Tobie, and K. Stahl, "Method for Calculating the Tooth Root Stress of Plastic Spur Gears Meshing With Steel Gears Under Consideration of Deflection-Induced Load Sharing," *Mechanism and Machine Theory* 111 (2017): 152–163.

13. A. Bravo, D. Koffi, L. Toubal, and F. Erchiqui, "Life and Damage Mode Modeling Applied to Plastic Gears," *Engineering Failure Analysis* 5 (2015): 113–133.

14. T. Itagaki, H. Takahashi, H. Iizuka, M. Takahashi, and R. Nemoto, Evaluating Fatigue Life of Injection-Molded-Plastic-Gear Added With Carbon Particle Made From Rice Hull, *3rd International Conference on Design Engineering and Science*, Pilsem, Czech Republic (2014).

15. P. Blais and L. Toubal, "Single-Gear-Tooth Bending Fatigue of HDPE Reinforced With Short Natural Fiber," *International Journal of Fatigue* 141 (2020): 105857.

16. D. Zorko, I. Demšar, and J. Tavčar, "An Investigation on the Potential of Bio-Based Polymers for Use in Gear Transmissions," *Polymer Testing* 93 (2021): 106994.

17. A. Bravo, L. Toubal, D. Koffi, and F. Erchiqui, "Gear Fatigue and Thermomechanical Behavior of Novel Green and Bio-Composite Materials vs High-Performance Thermoplastics," *Polymer Testing* 66 (2018): 403–414.

18. M. Hriberšek and S. Kulovec, "Preliminary Investigation of High-Density Polyethylene Reinforced With Spruce and Beech Fibers for Power Transmission Technologies," *Applied Composite Materials* 30 (2023): 1453–1476.

19. W. B. Ghazali, D. M. Idris, A. H. Sofian, M. F. bin Basrawi, and T. K. Ibrahim, Investigation on Wear Characteristics of Biopolymer Gear, *4th International Conference on Mechanical Engineering Research*, IOP Conference Series: Materials Science and Engineering (2017): 257.

20. B. Černe, M. Petkovšek, J. Duhovnik, and J. Tavčar, "Thermo-Mechanical Modeling of Polymer Spur Gears With Experimental Validation Using High-Speed Infrared Thermography," *Mechanism and Machine Theory* 146 (2020): 103734.

21. B. Černe and M. Petkovšek, "High-Speed Camera-Based Optical Measurement Methods for In-Mesh Tooth Deflection Analysis of Thermoplastic Spur Gears," *Materials and Design* 223 (2022): 111184.

22. F. Klocke, M. Brumm, and S. Herzhoff, "Influence of Gear Design on Tool Load in Bevel Gear Cutting," *Procedia CIRP* 1 (2012): 66–71.

23. G. Hlebanja, M. Erjavec, S. Kulovec, and J. Hlebanja, "Optimization of Planocentric Gear Train Characteristics With CA-Tools," in *New Approaches to Gear Design and Production. Mechanisms and Machine Science*, eds. V. Goldfarb, E. Trubachev, and N. Barmina, vol. 81 (Cham: Springer Nature, 2020), 323–347, https://doi.org/10.1007/978-3-030-34945-5_14.

24. ISO 1328-1: 2013 (en): Cylindrical Gears. ISO System of Flank Tolerance Classification. Part 1: Definitions and Allowable Values of Deviations Relevant to Flanks of Gear Teeth; International Organization for Standardization: Geneva (2013).

25. G. Mikoleizig, "Surface Roughness Measurements of Cylindrical Gears and Bevel Gears on Gear Inspection Machines," *Gear Technology* 5 (2015): 48–55.

26. VDI-RICHTLINIEN, VDI2736 Part 2: Thermoplastic Gear Wheels – Cylindrical Gears – Calculation of the Load Carrying Capacity, Beuth Verlag, Berlin (2014).

27. D. Grguraš, M. Kern, and F. Pušavec, "Cutting Performance of Solid Ceramic and Carbide end Milling Tools in Machining of Nickel Based Alloy Inconel 718 and Stainless Steel 316L," *APEM* 14 (2019): 27–38.

28. M. Hriberšek and S. Kulovec, "A Fundamental Approach to Determine the Impact of Aramid and Carbon Fibers on Durability and Tribological Performance of Different Polymer Composites Demonstrated in Gear Transmission Process," *Journal of Polymer Engineering* 43 (2023): 487–496.

29. VDI-RICHTLINIEN, VDI2736 Part 1: Thermoplastic Gear Wheels – Materials, Material Selection, Production, Methods, Production Tolerances, Form Design, Beuth Verlag, Berlin (2016).